Journal of Coordination Chemistry

Synthesis, structures, and catalytic oxidation of three aqua-coordinated and oxo-bridged diruthenium(III) complexes with sulfobenzoate and 2,2′-bipyridine

Wen-Ting Hu [a] & Long-Guan Zhu [a]

[a] Department of Chemistry , Zhejiang University , Hangzhou , P.R. China

PLEASE SCROLL DOWN FOR ARTICLE

Synthesis, structures, and catalytic oxidation of three aqua-coordinated and oxo-bridged diruthenium(III) complexes with sulfobenzoate and 2,2′-bipyridine

WEN-TING HU and LONG-GUAN ZHU*

Department of Chemistry, Zhejiang University, Hangzhou, P.R. China

Three new diruthenium(III) complexes, $[Ru_2O(2\text{-sb})_2(2,2'\text{-bipy})_2(H_2O)_2]\cdot 2.5H_2O$ (**1**), $[Ru_2O(3\text{-sb})_2(2,2'\text{-bipy})_2(H_2O)_2]\cdot 9H_2O$ (**2**), and $[Ru_2O(4\text{-sb})_2(2,2'\text{-bipy})_2(H_2O)_2]\cdot 9H_2O$ (**3**), where sb^{2-} is sulfobenzoate dianion and 2,2′-bipy is 2,2′-bipyridine, were synthesized using hydrothermal methods and characterized by IR, elemental analysis, thermogravimetric analysis, UV–vis, and fluorescence spectra. The single crystal X-ray analysis showed that each of these complexes has a dinuclear core stabilized by two bridging carboxylates and one bridging O^{2-}. Variable sb^{2-} ligands (2-sb, 3-sb, and 4-sb) in these complexes lead to diverse electronic spectroscopic behavior. The efficiency of activating methyl phenyl sulfide oxidation utilizing H_2O_2 in 3 equiv. was studied at $23 \pm 2\,°C$. The effect of the amount of catalyst and solvents on activities was investigated. Under optimized reaction conditions, the major product was sulfoxide. Complex **1** gave significant conversion of 100 and 98% selectivity for sulfoxide after 4 h.

Keywords: Diruthenium complex; Oxidation; Methyl phenyl sulfide; Sulfobenzoate

1. Introduction

Transition metal complexes are active catalysts [1–4]; Ru complexes containing nitrogen donors are important in a variety of catalytic reactions [5, 6]. These Ru complexes displayed satisfactory performance in olefin and ring-closing metathesis [7, 8], high chemo-selectivity [9], epoxidation [5], isomerization [10], ring-opening metathesis polymerization [11], and a wide range of redox reactions [9, 12–14]. Diruthenium complexes have been extensively studied due to their importance in structures and potential applications as functional materials [15, 16]. Ren and co-workers have developed a new class of diruthenium(II,III) complexes as catalysts used in the oxidation of methyl phenyl sulfide (MPS) [17, 18]. Some of them exhibit excellent catalytic activities. In the past decades, catalyzed oxidation of organic sulfides is important in fossil fuel desulfurization [19] and in medicinal chemistry [20, 21]. The reaction system of MPS, catalyst, and H_2O_2 is cheap, safe, neat, and environment friendly [22–25]. Mononuclear ruthenium complexes are inactive in oxidation of MPS [26]. We have been focusing on sulfobenzoate chemistry with two functional groups, carboxylate and sulfonate, for diverse coordination

---

*Corresponding author. Email: chezlg@zju.edu.cn

complexes [27–29]. The carboxylate of sb can be used to assemble dinuclear complexes. Herein, we report the synthesis and structures of a series of aqua-coordinated and oxo-bridged diruthenium complexes and their catalytic activities in oxidation of MPS, $[Ru_2O(2-sb)_2(2,2'-bipy)_2(H_2O)_2]·2.5H_2O$ **(1)**, $[Ru_2O(3-sb)_2(2,2'-bipy)_2(H_2O)_2]·9H_2O$ **(2)**, and $[Ru_2O(4-sb)_2(2,2'-bipy)_2(H_2O)_2]·9H_2O$ **(3)**, where 2,2′-bipy is 2,2′-bipyridine and sb^{2-} is sulfobenzoate dianion.

2. Experimental

2.1. *General procedures*

All chemicals were purchased from commercial sources in reagent grade and were used as received. Elemental analysis for C, H, and N were carried out on a Perkin–Elmer analyzer model 1110. Infrared spectra were obtained on a Nicolet Nexus 470 infrared spectrophotometer in KBr pellets from 400 to 4000 cm^{-1}. Fluorescence spectra were measured as powder samples using a Hitachi F-2500 FL spectrophotometer at room temperature. Thermogravimetric analyses were carried out using a Delta Series TA-SDT Q600 in nitrogen flow at a heating rate of 10 °C/min with Al_2O_3 crucibles. The UV–vis spectra were recorded on a SPECORD 2000 UV–vis spectrophotometer in CH_3OH at room temperature. The GC data were recorded on a Fuli Gas Chromatograph equipped with a DB-5 capillary column. All the standard substances used in GC were purchased from Alfa Aesar.

2.2. *Synthesis*

2.2.1. Synthesis of $[Ru_2O(2-sb)_2(2,2'-bipy)_2(H_2O)_2]·2.5H_2O$ (1). A mixture of $RuCl_3·3H_2O$ (0.032 g, 0.125 mM), 2-sulfobenzoic acid (0.076 g, 0.375 mM), 2,2′-bipyridine (0.020 g, 0.125 mM), and 18 mL H_2O was placed in a 30 mL Teflon-lined stainless steel reactor and heated at 403 K for 1 day. The vessel was slowly cooled to ambient temperature. A wine-red filtrate was obtained and dark red brick crystals of **1** were isolated, rinsed with distilled water and dried in the open air. Anal. Calcd (%) for $C_{34}H_{33}N_4O_{15.5}S_2Ru_2$: C, 40.36; H, 3.29; N, 5.54. Found: C, 40.27; H, 3.16; N, 5.5. IR (KBr, cm^{-1}): $v = 3431(s)$, 3114(w), 1555(s), 1472(w), 1448(w), 1408(s), 1239(s), 1186(s), 1145(w), 1086(w), 1020 (m), 771(m), 737(w), 727(w), 664(w), 616(m), 570(w), 478(w).

2.2.2. Synthesis of $[Ru_2O(3-sb)_2(2,2'-bipy)_2(H_2O)_2]·9H_2O$ (2). A mixture of $RuCl_3·3H_2O$ (0.032 g, 0.125 mM), 3-sulfobenzoic acid monosodium salt (0.112 g, 0.5 mM), 2,2′-bipyridine (0.020 g, 0.125 mM), and 18 mL H_2O was placed in a 30 mL Teflon-lined stainless steel reactor and heated at 403 K for 3 days. The vessel was slowly cooled to ambient temperature. A wine-red filtrate was obtained and blackish block crystals of **2** were isolated, rinsed with distilled water and dried in the open air. Anal. Calcd (%) for $C_{34}H_{46}N_4O_{22}S_2Ru_2$: C, 36.17; H, 4.11; N, 4.96. Found: C, 35.84; H, 3.93; N, 5.04. IR (KBr, cm^{-1}): $v = 3432(s)$, 3114(w), 1549(m), 1469(w), 1448(w), 1420(s), 1396(s), 1222 (m), 1187(s), 1166(s), 1103(m), 1080 (w), 1035(s), 997(w), 765(m), 724(w), 687(w), 674 (m), 618(m), 576(w), 490(w).

2.2.3. Synthesis of [Ru₂O(4-sb)₂(2,2′-bipy)₂(H₂O)₂]·9H₂O (3). A mixture of RuCl₃·3H₂O (0.064 g, 0.25 mM), 4-sulfobenzoic acid monopotassium salt (0.060 g, 0.25 mM), 2,2′-bipyridine (0.040 g, 0.25 mM), and 18 mL H₂O was placed in a 20 mL Teflon-lined stainless steel reactor and heated at 423 K for 1 day. The vessel was slowly cooled to ambient temperature and then filtered. A wine-red filtrate was obtained and allowed to evaporate. After two months, dark red brick crystals of **3** were obtained. Anal. Calcd (%) for $C_{34}H_{46}N_4O_{22}S_2Ru_2$: C, 36.17; H, 4.11; N, 4.96. Found: C, 36.56; H, 3.90; N, 4.81. IR (KBr, cm^{-1}): $\nu = 3423$(s), 3114(w), 1604(w), 1535(w), 1468(w), 1449(w), 1410(s), 1221 (s), 1190(s), 1118(s), 1034(s), 1010 (s), 855(w), 770(m), 741(s), 724(w), 697(w), 643(w), 560(w), 524(w).

2.3. *X-ray structure determination*

Single crystals of suitable size for X-ray diffraction were selected for data collection on a Bruker Smart CCD area detector with graphite-monochromated Mo-Kα radiation ($\lambda = 0.71073$ Å) at room temperature. For determination of the structures, the crystals were mounted on glass fibers in a random orientation. The structures were solved by the heavy atom method and successive Fourier syntheses. Fourier synthesis was performed to locate the other non-H atoms after the heavy atom peaks were located in the Patterson map. Full-matrix least-squares refinements on F^2 were carried out using the *SHELXL-97* package [30]. All non-H atoms were anisotropically refined. Complexes **2** and **3** were determined at low temperature. These three complexes contain a large number of lattice waters, and therefore the data were processed using the SQUEEZE algorithm included in PLATON. WinGX and PLATON software were used for structural solution, refinement, and drawing [31, 32]. The detailed crystallographic data and refinement parameters for **1–3** are listed in table 1.

CCDC 913720–913722 for **1–3** contain Supplementary crystallographic data for this paper. These data can be obtained free of charge from the Cambridge Crystallographic Data Center via www.ccdc.cam.ac.uk/data_request/cif.

2.4. *Catalytic reaction*

The catalytic procedure is similar to that of Monge, except that we did the reaction at ambient temperature (23 ± 2 °C) [33]. A 20 mL round-bottom flask was charged with a suspension of the catalyst (0.02, 0.04, or 0.06 mM) in organic solvent (6 mL) and the substrate MPS (2 mM). The mixture was stirred at room temperature for 10 min. Reaction was started by the addition of the corresponding amount of H_2O_2 solution (30%, 6 mM) under stirring. The first sample was taken after 10 min and the later samples were taken at specified time with a fixed interval of 1 h and analyzed by gas chromatography. The catalyzed reactions were continued for 310 min.

3. Results and discussion

3.1. *Molecular structures*

Complexes **1–3** are dinuclear structures with a neutral core of [Ru₂(µ-oxo) (sb)₂(H₂O)₂(2,2′-bipy)₂] (scheme 1). Each ruthenium in the dinuclear core is coordinated

Table 1. Crystallographic data and refinement parameters for **1–3**.

Complex	**1**	**2**	**3**
Empirical formula	$C_{68}H_{66}N_8O_{31}Ru_4S_4$	$C_{34}H_{46}N_4O_{22}Ru_2S_2$	$C_{34}H_{46}N_4O_{22}Ru_2S_2$
Mr	1932.76	966.88	966.88
Crystal system	Orthorhombic	Trigonal	Triclinic
Space group	$Pca2_1$	$P6_3/m$	$P\text{-}1$
Size (mm^3)	$0.09 \times 0.19 \times 0.50$	$0.23 \times 0.28 \times 0.32$	$0.04 \times 0.06 \times 0.37$
a (Å)	20.001(3)	17.9396(8)	12.3274(6)
b (Å)	14.875(3)	17.9396	13.6837(6)
c (Å)	24.916(4)	23.2440(13)	14.6523(7)
α (°)	90	90	76.569(1)
β (°)	90	90	65.901(1)
γ (°)	90	120	81.732(1)
V (Å^3)	7412.9(19)	6478.39(5)	2176.74(12)
Z	4	6	2
D_c (Mg m^{-3})	1.732	1.487	1.475
μ (mm^{-1})	0.999	0.857	0.850
θ range	1.6–25.5	1.3–25.1	1.5–25.0
Unique reflections	13,595	3953	7569
Observed reflections	11,480	2681	5616
Parameters	1016	273	544
F (000)	3868	2904	968
T(K)	295(2)	173(2)	173(2)
R_1	0.039	0.053	0.055
wR_2 [$I>2\sigma(I)$]	0.090	0.133	0.171
R_1	0.051	0.082	0.074
wR_2 [all data]	0.096	0.150	0.189
GOF	0.993	0.965	0.990

by two N from two 2,2′-bipy, one bridging O dianion, two O atoms from two sb, and one O atom from water (figures 1–3). All sb ligands are completely deprotonated, thus the metal oxidation state is $+3$. The structural parameters of Ru–O(oxo), Ru–O(COO), Ru$\cdots$Ru distances, and Ru–O–Ru angles (table 2) in these complexes fall in a similar range and are in good agreement with those reported in the literature [34–38]. The variable sulfobenzoates do not remarkably influence these structural parameters.

In these three complexes there are $\pi\cdots\pi$ interactions between pyridine rings from neighboring dicores, and abundant C–H$\cdots\pi$ interactions. Hydrogen-bonding interactions consolidate these complexes into 3-D architectures, enhancing the structure stability.

Although these complexes have similar structural parameters, the arrangement of the two sb in these dicores is somewhat different. Complex **2** has a mirror plane and two sulfonates are *cis*. The dihedral angle of two benzene rings is 81.5(2)° in **2**. In **1**, there are two dicore units in an asymmetric unit and these two units have different arrangement for two sb ligands (figure 1) with dihedral angles of 9.7(5)° and 85.6(2)°, respectively. In **3**, the dihedral angle for two sb is 89.1(3)°. Furthermore, the arrangement of the 2,2′-bipy and the sb *trans* to oxo is different in these complexes, indicating that the substituent groups on the sb can tune the steric arrangement of ligands in these dicores.

Our dicore complexes have some differences with Ren's paddlewheel complexes [17, 18]: (1) metal ions in both types have different oxidation states; (2) our structures are supported by oxide bridge; and (3) Ren's complexes have a short Ru$\cdots$Ru distance. Over 40 dicore complexes with oxo-bridges have been reported from the search of CSD (Version 5.34-Feb 2013) [39] and a few complexes with aqua-coordination were synthesized [40, 41]. Dicore ruthenium complexes with carboxylate bridging ligands as
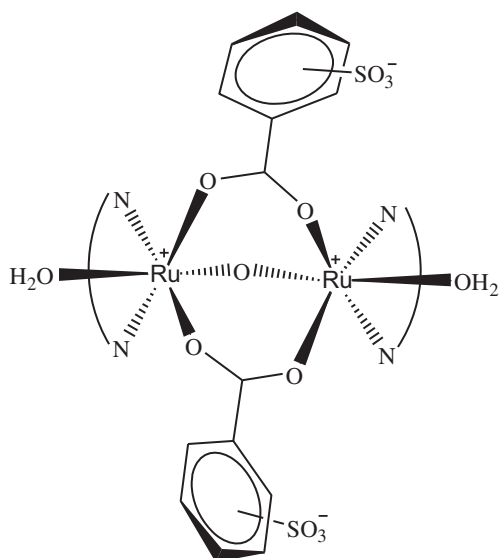
Scheme 1. General drawing of aqua-coordinated and oxo-bridged diruthenium(III) complexes. ⌢N N = 2,2′-bipyridine.
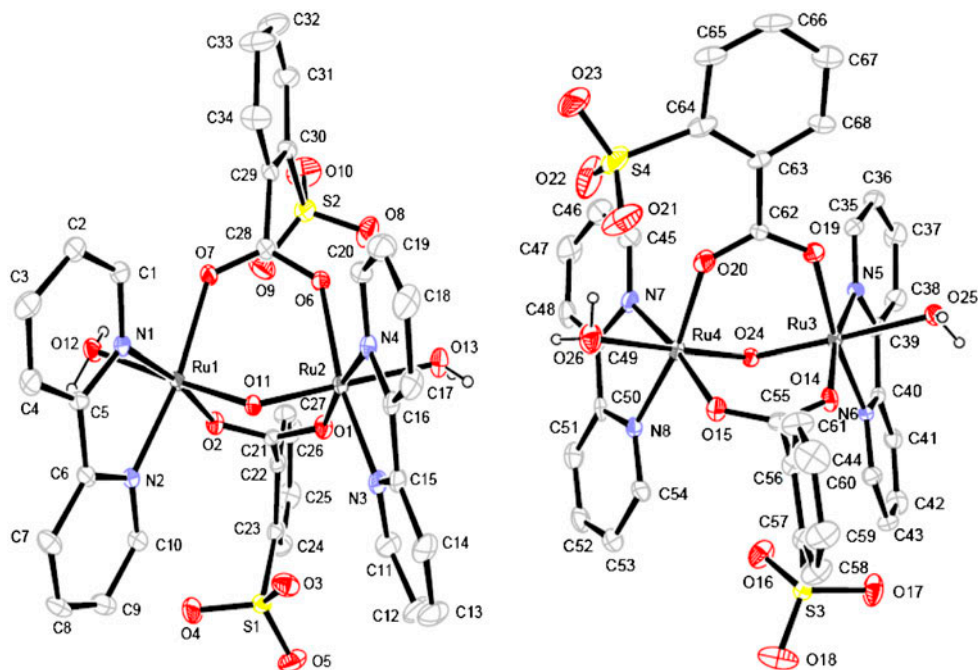
Figure 1. ORTEP view of two diruthenium cores in **1**. Hydrogens on C and lattice waters are omitted for clarity.
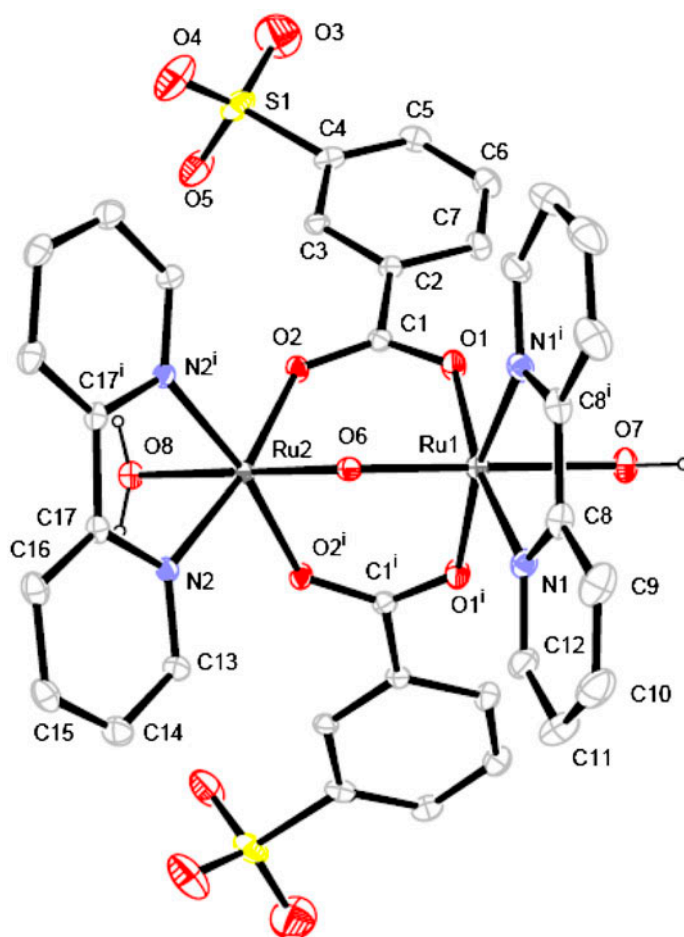
Figure 2.   ORTEP view of the diruthenium core in **2**. Hydrogens on C and lattice waters are omitted for clarity.
Symmetry code: $I = x$, y, $1.5 - z$.

dianion have never been recorded, thus our dicore complexes with oxo-bridge and
aqua-coordination are a new type of diruthenium complex.

3.2. *Thermal stability*

Thermal stabilities of the three complexes were studied as shown in Supplementary
material. TG analysis of **1** shows a three-step weight loss of 8.14%, corresponding to the
release of lattice water and two coordinated waters (calculated 8.01%) from room
temperature to 220 °C. For **2**, from room temperature to 230 °C, the weight loss of 18.18%
was attributed to the loss of lattice water and two coordinated waters (calculated 17.55%).
Complex **2** started to decompose at 326 °C. For **3**, nine lattice waters were lost from room
temperature to 140 °C (calculated 14.36%, observed 14.73%). In the second step, the
weight loss of 2.92% was ascribed to the release of two coordinated waters (calculated
3.19%).
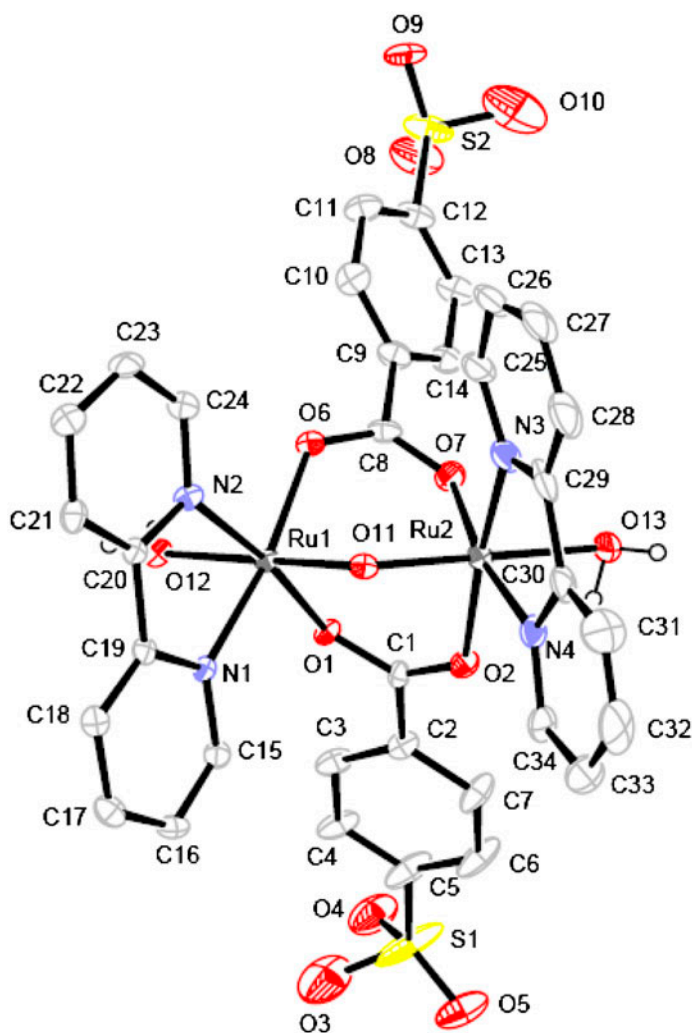
Figure 3. ORTEP view of the diruthenium core in **3**. Hydrogens on C and lattice waters are omitted for clarity.

3.3. *UV–vis spectra*

UV–vis spectra in methanol of **1–3** and 2-H$_2$sb, 3-NaHsb, 4-KHsb, and 2,2′-bipy at room temperature were measured. The spectra of the complexes are shown in supplementary material and the data are listed in table 3. The data for ligands are listed in table S1. Complexes **1–3** have their strongest bands at 221, 234, and 214 nm, respectively, which are attributed to π–π^* transitions. It is interesting to compare the properties of diruthenium complexes with corresponding ligands. Structures **1** and **2** do not have evident shift compared with 2-H$_2$sb at 221 nm and 3-NaHsb at 228 nm, respectively. However, **3** has the strongest absorption at 214 nm, which, by contrast, has a distinct blue shift in comparison with 4-KHsb at 234 nm. This may be ascribed to the para sulfonate in **3,** playing an important role in conjugation, although the electronic effect of the ortho-position of **1** and para-position of **4** are similar. Better conjugation results are seen in a lower energy level of

Table 2.   Selected bond lengths (Å) and angles (°).

Complex 1

Ru1–O2	2.074(4)	Ru1–O7	2.090(4)	Ru1–O11	1.857(4)
Ru1–O12	2.134(4)	Ru1–N1	2.044(5)	Ru1–N2	2.024(5)
Ru2–O1	2.098(4)	Ru2–O6	2.071(4)	Ru2–O11	1.862(4)
Ru2–O13	2.111(5)	Ru2–N3	2.041(6)	Ru2–N4	2.027(5)
Ru1–Ru2	3.2625(7)	Ru3–O14	2.073(4)	Ru3–O19	2.092(4)
Ru3–O24	1.862(4)	Ru3–O25	2.135(4)	Ru3–N5	2.022(5)
Ru3–N6	2.020(5)	Ru4–O15	2.090(4)	Ru4–O20	2.073(5)
Ru4–O24	1.862(4)	Ru4–O26	2.130(5)	Ru4–N7	2.019(5)
Ru4–N8	2.047(5)	Ru3–Ru4	3.2275(7)		
N1–Ru1–N2	79.9(2)	N1–Ru1–O2	169.88(18)	N1–Ru1–O7	94.17(19)
N1–Ru1–O11	91.97(18)	N1–Ru1–O12	85.40(18)	N2–Ru1–O2	93.14(19)
N2–Ru1–O7	170.82(19)	N2–Ru1–O11	91.05(19)	N2–Ru1–O12	89.68(19)
O2–Ru1–O7	91.77(17)	O2–Ru1–O11	95.53(17)	O2–Ru1–O12	87.23(18)
O7–Ru1–O11	96.19(17)	O7–Ru1–O12	82.82(17)	O11–Ru1–O12	177.11(19)
N3–Ru2–O1	96.9(2)	N3–Ru2–O6	169.72(19)	N3–Ru2–O11	91.2(2)
N3–Ru2–O13	87.4(2)	N3–Ru2–N4	79.0(2)	N4–Ru2–O1	174.01(19)
N4–Ru2–O6	95.7(2)	N4–Ru2–O11	89.15(19)	N4–Ru2–O13	88.7(2)
O1–Ru2–O6	87.72(18)	O1–Ru2–O11	95.33(17)	O1–Ru2–O13	86.77(19)
O6–Ru2–O11	97.50(17)	O6–Ru2–O13	83.66(19)	O11–Ru2–O13	177.6(2)
Ru1–O11–Ru2	122.6(2)				

Complex 2

Ru1–O1	2.070(4)	Ru1–O6	1.843(5)	Ru1–O7	2.153(6)
Ru1–N1	2.019(5)	Ru2–O2	2.070(4)	Ru2–O6	1.843(6)
Ru2–O8	2.145(7)	Ru2–N2	2.047(4)		
Ru1–Ru2	3.2608(9)	Ru2–O6–Ru1	123.7(3)		

Complex 3

Ru1–O1	2.089(4)	Ru1–O6	2.093(4)	Ru1–O11	1.847(4)
Ru1–O12	2.125(4)	Ru1–N1	2.017(5)	Ru1–N2	2.029(5)
Ru2–O2	2.067(4)	Ru2–O7	2.113(5)	Ru2–O11	1.876(4)
Ru2–O13	2.115(5)	Ru2–N3	2.043(6)	Ru2–N4	2.013(6)
Ru1–Ru2	3.2130(7)				
O1–Ru1–O6	90.53(19)	O1–Ru1–O11	95.4(2)	O1–Ru1–O12	85.77(19)
O1–Ru1–N1	94.8(2)	O1–Ru1–N2	171.7(2)	O6–Ru1–O11	93.4(2)
O6–Ru1–O12	87.0(2)	O6–Ru1–N1	171.5(2)	O6–Ru1–N2	94.3(2)
O11–Ru1–O12	178.7(2)	O11–Ru1–N1	92.6(2)	O11–Ru1–N2	91.0(2)
O12–Ru1–N1	86.8(2)	O12–Ru1–N2	87.8(2)	N1–Ru1–N2	79.6(2)
Ru1–O11–Ru2	119.3(2)				

Table 3.   UV–vis absorption spectral data of **1–3** in CH_3OH ($C = 1.25 \times 10^{-5} \, M \, L^{-1}$).

Complex	λ_{max}/nm		(ε/dm^3 M^{-1} cm^{-1})	
1	221 (184,975)	275 (77,312)	299 (51,894)	600 (20,935)
2	234 (202,573)		300 (26,229)	600 (8224)
3	214 (49,580)	250 (35,812)	305 (48,060)	506 (8134)

the basic state of an electron. Consequently, the energy level difference is bigger and a blue shift takes place in **3**.

The band at 275 nm of **1** and 250 nm of **3** are the results of MLCT. Nevertheless, **2** does not have a charge transfer band between 250 and 300 nm. This may be because the electronic effect of 3-sb is different from those of 2-sb and 4-sb.

Complexes **1–3** exhibit absorptions at 299, 300, and 305 nm, respectively, which come from 2,2'-bipyridine. These bands demonstrate that the red shift arises after 2,2'-bipyridine coordinates to ruthenium. Furthermore, these bands are stronger than that of free 2,2'-bipy, indicating that coordination enhances the absorptions.

There are weak visible bands at 600, 600, and 506 nm for **1**, **2,** and **3**, respectively, attributed to the charge transfer of Ru(III)–dπ and μ–O–pπ orbitals. According to Syamala and co-workers [41], these bands come from the (μ-oxo)bis(μ-carboxy1ato)diruthenium(III) core. Abe's dicore complexes exhibit strong absorption in this range [42], while Ren's dicore complexes have no absorption in this range [17]. Obviously, there are some effects of the positions of the substituents on the bridging sulfobenzoate ligands, somewhat different from those of reported diruthenium core complexes.

3.4. *Fluorescence spectra*

Fluorescent properties of **1–3** in the solid state at room temperature ($\lambda_{ex} = 240$ nm) are almost the same as shown in figure 4; data are listed in table S2. Emission spectra ($\lambda_{ex} = 240$ nm) of 2-H$_2$sb, 3-NaHsb, 4-KHsb, and 2,2'-bipy were also measured and listed in table S3. Their strong emission centered at 388.5 nm is generated from the π–π^* ligand centered charge transfer (LC) of sb and 2,2'-bipy. They showed weak emission at 292 nm, which is primarily from 2,2'-bipy. From the emission spectra of free 2-sb, 3-sb, and 4-sb, we can see subtle differences in their peaks. Nevertheless, the photochemical properties of the three complexes are in accord with each other, indicating that the chelating of sb to ruthenium does not have a significant effect on their fluorescence behavior. The order of emission intensity is **3 > 1 > 2**.
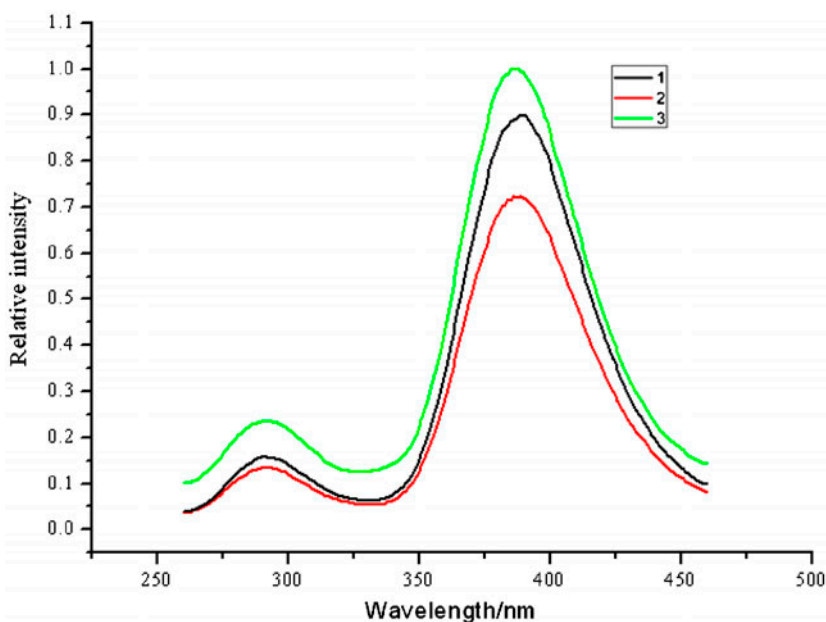

Figure 4.   Fluorescent spectra of **1–3** in the solid state ($\lambda_{ex} = 240$ nm).

3.5. *Oxidation catalysis*

For insight into the factors that affect the efficiency of MPS oxidation (scheme 2), we examined the molar ratio of reagents, solvents, amount of oxidant, and catalysts. Preliminary evaluation of the three complexes is displayed in table 4. MPS was consumed to produce sulfoxide (dominant) and sulfone. From table 4, we can see that **1** has the highest efficiency in promoting MPS oxidation. MPS was consumed by 95% to yield the corresponding sulfoxide (90%) and sulfone (10%). Consequently, **1** was chosen to examine the amount of H_2O_2 as well as catalyst and the impact of different solvents on the oxidation efficiency.

The effect of catalyst amount on the oxidation efficiency was investigated using **1**. Table 5 shows the results with catalyst loading at 1, 2, and 3% to the amount (M) of MPS, respectively. The performance in the presence of 1% of catalyst was slowest. Surprisingly, 2% displayed comparative performance with 3%. Conversion and selectivity for sulfoxide are 97 and 92%, when catalyst loading is 3%, showing almost the same activity with 2% loading. Taking into consideration that cost and efficiency are the key factors in commercial applications, we decided to choose the 2% loading as the optimal amount of catalyst. Subsequently, the impact of different solvents on organic sulfide oxidation was investigated with catalyst loading 2% to substrate, while other reaction conditions were the same as above. As shown in table 6, most efficient performance was observed in ethanol, which showed a small advantage in rate and selectivity in comparison with methanol. Acetonitrile, which was frequently seen in reports on oxidation of organic sulfides [43], was less effective. Acetone was perplexing with moderate conversion achieved in the first 70 min, but little change was detected thereafter. The oxidation stopped because of oxidant consumption involving reaction with acetone, giving the triacetone-triperoxide or diacetone-diperoxide products reported by several groups (Caution! During handling of the triacetone-triperoxide or diacetone-diperoxide care should be taken because of the possibility of explosion and only small amount of acetone was used in such
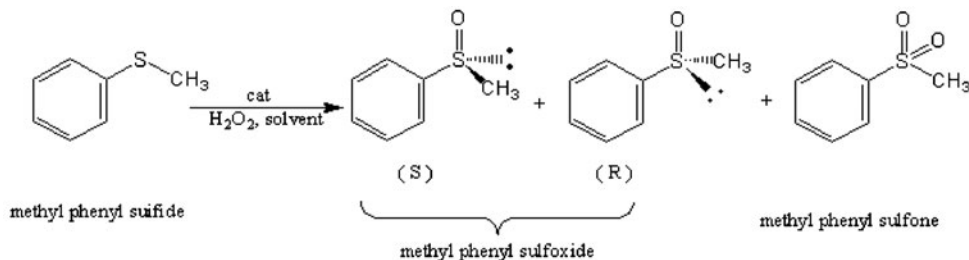
Scheme 2.   The oxidation of MPS.

Table 4.   Preliminary assessment of catalytic activity of the three complexes.

Complex	t/min	Conversion (%)	Selectivity for sulfoxide (%)
1	310	95	90
2	310	24	89
3	310	58	94

Note: In each reaction, 2 mM of MPS, 0.02 mM of catalyst and 3 equiv. of H_2O_2 were mixed in 6 mL of acetonitrile at ambient temperature ($23 \pm 2\,^{\circ}$C). Samples were taken at specified time, processed, and analyzed by GC.

Table 5. Oxidation efficiency with different catalyst loading of **1**.

Catalyst loading (to MPS) (%)	t/min	Conversion (%)	Selectivity for sulfoxide (%)
1	310	88	93
2	310	97	91
3	310	97	92

Note: In each reaction, 2 mM of MPS, specific amount of **1** and 3 equiv. of H_2O_2 were mixed in 6 mL of acetonitrile at ambient temperature ($23 \pm 2\,°C$). Samples were taken at specified time, processed, and analyzed by GC.

Table 6. Oxidation efficiency in different solvents of **1**.

Solvent	t/min	Conversion (%)	Selectivity for sulfoxide (%)
CH_3CN	310	97	91
Methanol	250	100	92
Ethanol	190	99	93
Acetone	310	55	77

Note: In each reaction, 2 mM of MPS, 0.04 mM of **1** and 3 equiv. of H_2O_2 were mixed in 6 mL of specific solvent at ambient temperature ($23 \pm 2\,°C$). Samples were taken at specified time, processed, and analyzed by GC.

experiment) [44]. The efficiency in CH_2Cl_2 was also examined, but conversion was unexpectedly low. Consequently, ethanol was used as solvent in MPS oxidation. The optimal reaction conditions are 2 mM of MPS, 0.04 mM of catalyst, and 3 equiv. of H_2O_2 were mixed in 6 mL of specific solvent at ambient temperature ($23 \pm 2\,°C$). A blank reaction in the absence of any catalyst under otherwise identical reaction conditions was also carried out (figure 5), and the results showed that only H_2O_2 could produce a small quantity of products.
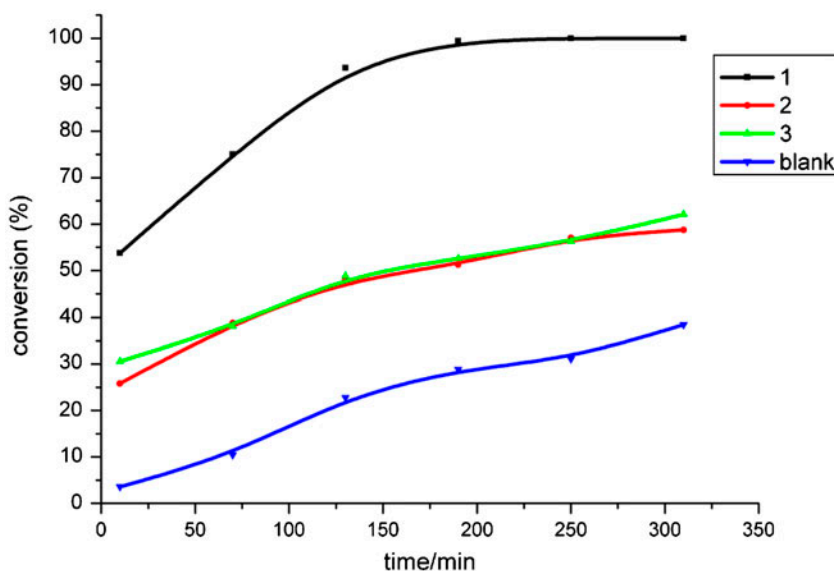

Figure 5. Conversion *vs.* time for oxidation with 2 mM MPS, 2% of catalysts **1–3** (based on the substrate) and 3 equiv. of H_2O_2 in 6 mL of CH_3CH_2OH at $23 \pm 2\,°C$. Blank was absence of catalyst otherwise the same.

The three complexes have an order of $1 > 3 > 2$ showing large disparity in conversion (figure 5). MPS was totally consumed after 4 h in the presence of **1**. In the case of **3**, conversion of 62% was observed after 310 min and 59% of the MPS was consumed with **2**. **1** was the most prominent in catalyzed oxidation, suggesting that the ortho position of the sulfo group provides better conjugation leading to dominance in catalyzed oxidation. Electron richness of the (μ-oxo)bis(μ-carboxy1ato)diruthenium(III) core stems from the approach of sulfoxylato to the dicore center. In terms of selectivity for sulfoxide, **1–3** are comparable with 96–98%, suggesting that diruthenium complexes are superior in conversion and selectivity for sulfoxide. Compared with inactive catalysis of mononuclear ruthenium complexes, dicore ruthenium complexes exhibit excellent catalytic activities. Complex **1** is superior in conversion with 100% in 4 h and has 98% selectivity for sulfoxide after 310 min.

Our dimeric complexes exhibit efficient catalytic activity and are also better than those of Mo, Mn, and W complexes [24, 25, 45]. While the detailed mechanism of the Ru dimers remains unknown [17], Ren and co-workers considered that it is likely that the Ru_2 unit activates the peroxy species using an axial position.

4. Conclusion

A new class of diruthenium complexes with coordination of both aqua and oxo bridges were synthesized. Each for Ru in these complexes has an oxidation state of +3 and adopts a distorted octahedral geometry. The variation of substituting positions of sb^{2-} in the ligands results in distinct electronic absorptions. These complexes were utilized as catalysts for sulfide oxidation using H_2O_2 at ambient temperature under optimized reaction conditions. In comparison with the blank reaction, they displayed excellent efficiency in conversion and selectivity. Furthermore, **1** was effective in rate and conversion, indicating that it is a candidate for organic sulfide oxidation.

Supplementary material

Data of UV–vis spectra of ligands in the methanol (table S1); Fluorescence spectral data of **1–3** in solid state (table S2); Fluorescence spectral data of ligands in solid state (table S3); TG curves for **1–3** (figure S1); UV–vis absorption spectra of **1–3** in CH_3OH (figure S2); Crystallographic data in CIF format (CCDC of 913720, 913721, and 913722).

Acknowledgements

References

[1] A. Zarkadoulas, E. Koutsouri, C.A. Mitsopoulou. *Coord. Chem. Rev.*, **256**, 2424 (2012).
[2] S. Krompiec, M. Penkala, K. Szczubialka, E. Kowalska. *Coord. Chem. Rev.*, **256**, 2057 (2012).
[3] J. Barbier-Jr, F. Delanoe, F. Jabouille, D. Duprez, G. Blanchard, P. Isnard. *J. Catal.*, **177**, 378 (1998).
[4] L. Bernet, R. Lalrempula, W. Ghattas, H. Mueller-Bunz, L. Vigara, A. Llobet, M. Albrecht. *Chem. Commun.*, **47**, 8058 (2011).

[5] M. Dakkach, X. Fontrodona, T. Parella, A. Atlamsani, I. Romero, M. Rodriguez. *Adv. Synth. Catal.*, **353**, 231 (2011).

[6] L.T. Ghoochany, A. Farsadpour, Y. Sun, W.R. Thiel. *Eur. J. Inorg. Chem.*, **3431**, (2011).

[7] M. Scholl, S. Ding, C.W. Lee, R.H. Grubbs. *Org. Lett.*, **1**, 953 (1999).

[8] M. Ahmed, A.G.M. Barrett, D.C. Braddock, S.M. Cramp, P.A. Procopiou. *Tetrahedron Lett.*, **40**, 8657 (1999).

[9] M.J. Burk, W. Hems, D. Herzberg, C. Malan, A. Zanotti-Gerosa. *Org. Lett.*, **2**, 4173 (2000).

[10] C. Cadot, P.I. Dalko, J. Cossy. *Tetrahedron Lett.*, **43**, 1839 (2002).

[11] D.R. Wang, J. Unold, M. Bubrin, W. Frey, W. Kaim, M.R. Bachmeiser. *ChemCatChem*, **4**, 1808 (2012).

[12] S. Horn, M. Albrecht. *Chem. Commun.*, **47**, 8802 (2011).

[13] L. Roecker, J.C. Dobson, W.J. Vining, T.J. Meyer. *Inorg. Chem.*, **26**, 779 (1987).

[14] B. Radaram, J.A. Ivie, W.M. Singh, R.M. Grudzien, J.H. Reibenspies, C.E. Webster, X. Zhao. *Inorg. Chem.*, **50**, 10564 (2011).

[15] L. Neubert, D. Michalik, S. Bahn, S. Imm, H. Neumann, J. Atzrodt, V. Derdau, W. Holla, M. Beller. *J. Am. Chem. Soc.*, **134**, 12239 (2012).

[16] T.L. Zhang, C.P. Ji, K.L. Wang, D. Fortin, P.D. Harvey. *Inorg. Chem.*, **49**, 11069 (2010).

[17] L. Villalobos, Z. Cao, P.E. Fanwick, T. Ren. *Dalton Trans.*, 644 (2012).

[18] J.E. Barker, T. Ren. *Inorg. Chem.*, **47**, 2264 (2008).

[19] B. Delmon. *Catal. Lett.*, **22**, 1 (1993).

[20] W. Adam, M.N. Korb, K.J. Roschmann, C.R. Saha-Moller. *J. Org. Chem.*, **63**, 3423 (1998).

[21] O. Hamelin, P. Guillo, F. Loiseau, M.F. Biossonnet, S. Menage. *Inorg. Chem.*, **50**, 7952 (2011).

[22] C. Bolm, F. Bienewald. *Angew. Chem. Int. Ed. Engl.*, **34**, 2640 (1995).

[23] H.M. Shi, C.G. Yu, J. He. *J. Catal.*, **271**, 79 (2010).

[24] N.Y. Jin. *J. Coord. Chem.*, **65**, 4013 (2012).

[25] M. Amini, M. Bagherzadeh, Z. Moradi-Shoeili, D.M. Boghaei, A. Ellern, L.K. Woo. *J. Coord. Chem.*, **66**, 464 (2013).

[26] I. Claustro, G. Abate, E. Sanchez, J.H. Acquaye. *Inorg. Chim. Acta*, **342**, 29 (2003).

[27] X.F. Zheng, L.G. Zhu. *Cryst. Growth Des.*, **9**, 4407 (2009).

[28] X.F. Zheng, L.G. Zhu. *Cryst. Eng. Comm*, **12**, 2878 (2010).

[29] X.H. Miao, L.G. Zhu. *Dalton Trans.*, 1457 (2010).

[30] G.M. Sheldrick. *SHELXL-97, Program for Crystal Structure Refinement*, University of Göttingen, Göttingen (1997).

[31] L. Farrugia. *J. Appl. Crystallogr.*, **32**, 837 (1999).

[32] A.L. Spek. *Acta Crystallogr.*, **D65**, 148 (2009).

[33] F. Gandara, C. Fortes-Revilla, N. Snejko, E. Gutierrez-Puebla, M. Iglesias, M.A. Monge. *Inorg. Chem.*, **45**, 9680 (2006).

[34] Y. Sasaki, M. Suzuki, A. Tokiwa, E. Ebihara, T. Yamaguchi, C. Kabuto, T. Ito. *J. Am. Chem. Soc.*, **110**, 6251 (1988).

[35] A. Llobet, M.E. Curry, H.T. Evans, T.J. Meyer. *Inorg. Chem.*, **28**, 3131 (1989).

[36] Y. Sasaki, M. Suzuki, A. Nagasawa, A. Tokiwa, M. Ebihara, T. Yamaguchi, C. Kabuto, T. Ochi, T. Ito. *Inorg. Chem.*, **30**, 4903 (1991).

[37] N. Gupta, S. Mukerjee, S. Mahapatra, M. Ray, R. Mukherjee. *Inorg. Chem.*, **31**, 139 (1992).

[38] C. Sudha, A.R. Chakravarty. *J. Chem. Soc., Dalton Trans.*, 3289 (1996).

[39] F.H. Allen. *Acta Crystallogr., Sect. B: Struct. Sci*, **58**, 380 (2002).

[40] A. Hassain, A.K. Bhatt, D.K. Kumar, R.B. Thorat, H.J. Padhiyar, R.S. Shukla. *Inorg. Chim. Acta*, **362**, 1101 (2009).

[41] A. Syamala, A.R. Chakravarty. *Inorg. Chem.*, **30**, 4699 (1991).

[42] H.X. Zhang, K. Tsuge, Y. Sasaki, M. Osawa, M. Abe. *Eur. J. Inorg. Chem.*, **2011**, 5132 (2011).

[43] H.B. Lee, T. Ren. *Inorg. Chim. Acta*, **362**, 1467 (2009).

[44] F. Dubnikova, R. Kosloff, J. Almog, Y. Zeiri, R. Boese, H. Itzhaky, A. Alt, E. Keinan. *J. Am. Chem. Soc.*, **127**, 1146 (2005).

[45] M. Amini, M. Bagherzadeh, B. Eftekhari-Sis, A. Ellern, L.K. Woo. *J. Coord. Chem.*, **66**, 1897 (2013).